CIT. Journal of Computing and Information Technology, Vol. 32, No. 4, December 2024, 235–250
doi: 10.20532/cit.2024.1005860

Enhanced YOLOv5s for PCB Defect Detection with Coordinate Attention and Internal Convolution

Zhijun Xiao

School of Electrical and Electronic Information Engineering, Hubei Polytechnic University, Huangshi, Hubei, China

Printed Circuit Board (PCB) defect detection is crucial for ensuring the quality and reliability of electronic devices. The study proposes an enhanced YOLOv5s model for PCB defect detection, which combines Coordinate Attention (CA), Convolutional Block Attention Module (CBAM), and Inception-style convolutions (IO). This model aims to improve the detection accuracy of small defects while reducing computational complexity. Experiments on the PCB defect dataset demonstrate that the proposed CA-CBAM-IO-YOLOv5s model achieves higher accuracy (97.8%), recall (98.6%), and F1 score (98.3%) compared to the basic YOLOv5s and other state-of-the-art models. The model also shows excellent performance in detecting various types of PCB defects, with an average detection accuracy of 98.45% and an average detection time of 0.114 seconds. These results indicate that the proposed model provides a promising solution for efficient and accurate PCB defect detection in industrial applications.

ACM CCS (2012) Classification: Applied computing → Physical sciences and engineering → Electronics

Keywords: PCB, YOLOv5s, CA, CBAM, defect detection, IO

1. Introduction

In today's digital age, electronic products have become an indispensable part of our lives. From smartphones and computers to complex medical devices and spacecraft, the functionality and reliability of these devices depends in large part on a key component inside them − the printed circuit board (PCB). PCB is the cornerstone of electronic components, they not only carry the transmission of electronic signals, but also support the physical structure of each component [1−2]. Therefore, the quality of the PCB is directly related to the performance, stability and safety of the entire electronic product. However, PCB defects such as signal interference, overheating, power fluctuations, wire breaks or short circuits can seriously threaten the performance and reliability of electronic products. For example, improper design may lead to incorrect data transmission of communication devices, heat dissipation problems may shorten the service life of medical devices, and short circuits may even cause fires, posing a direct threat to user safety. Therefore, how to efficiently and accurately detect these defects has become a key research issue in the field of electronic manufacturing. Traditional PCB inspection methods mainly rely on manual visual inspection and electrical testing, but these methods have problems like low efficiency, poor accuracy, and high cost [3−4]. With the rapid growth of computer vision and deep learning (DL) technology, image processing-based non-destructive testing technology has gradually become an important means of PCB detection. The use of DL to detect defects in electronic devices has become a popular research topic at present. Among them, compared to other algorithms in the field of object detection, the You Only Look Once (YOLO) series of algorithms have been widely applied. This series of algorithms transforms object detection into a single pipeline, enabling rapid detection of multiple targets within an image, thus efficiently and accurately completing the detection

task. With the progress of the YOLO series, the YOLOv5s algorithm inherits the core concept of the YOLO series and improves the detection performance and efficiency of first-generation YOLO by optimizing network structure and data augmentation technology [5]. To further improve the effectiveness of PCB-Defect Detection (PCBDD), this study proposes an improved YOLOv5s model that combines Coordinate Attention (CA), Convolutional Block Attention Mechanisms (CBAM), and Convolutional Operator (IO) mechanisms. The innovation lies in the addition of the CA mechanism to capture the feature position information of the model in the spatial dimension, and the addition of CBAM to improve the representation ability of the feature map. Meanwhile, IO is also utilized to reduce computational complexity and parameter count. This study is not only expected to provide new technical means for PCBDD, but also valuable references for other similar object detection tasks.

2. Related Works

PCBDD refers to the detection of surface and internal defects in PCBs through various technical means to ensure their quality and performance. Through defect detection, not only can defects be detected and corrected in a timely manner during the production process, but it can also reduce production costs, improve product reliability and production quality. With the development of machine learning techniques, several studies have begun to explore the use of these algorithms to improve the automation and accuracy of detection. For example, Zhou *et al.* proposed a PCB defect detection algorithm that optimizes YOLOv5 networks based on multi-scale attention mechanisms. The research results show that this method reduces the number of parameters of the traditional v5 algorithm (You only look once version 5, YOLOv5s) by 46% and improves the detection accuracy by 3.34% [6].

Deep learning, especially convolutional neural networks, has become a leading technology in PCB defect detection. Yu *et al.* designed a lightweight and efficient network for the detection of tiny defective objects to solve the problems of small objects' small size and blurred pixels. In the backbone network, the diagonal feature pyramid is proposed, and the precision of network detection is improved by the same level feature fusion. At the same time, computational costs are reduced by eliminating bottom-up paths and removing some features. In the neck network, a multi-scale neck network is designed to adapt to multi-scale micro defect detection, and an adaptive localization loss function is introduced to improve sensitivity. The final results show that this model is superior to mainstream detection algorithms in both accuracy and speed [4]. Sezer *et al.* proposed an optimized deep learning model to improve PCB defect detection accuracy. A two-dimensional signal processing method was developed to detect solder paste defects on PCB efficiently at an early stage. In addition, the model uses convolutional neural networks to classify solder joint regions on the PCB. The experimental results show that the model has successfully detected and visualized the defective solder paste area on PCB by combining image processing and deep learning methods [7].

To further improve detection performance, researchers have proposed a variety of improved deep learning models. Long *et al.* propose an improved YOLO algorithm in which not only ShuffleAttention and BiFPN structures are added, but also WIoU loss functions are used instead of traditional CIoU loss functions to improve detection accuracy and robustness. Experimental results show that the proposed improved algorithm achieves 94.2% and 49.0% respectively on mAP50 and mAP90-95, and the number of parameters and weight size are reduced by 33% and 32% respectively, showing good performance [8]. Aiming at the complexity of industrial surface defect detection, Xie *et al.* proposed an algorithm based on feature enhancement YOLO. The YOLO model is first simplified by combining deep separable convolution and dense joins. Secondly, the feature pyramid network is improved to improve the precision of multi-scale detection layer. Finally, the new prediction frame regression loss function and K-means algorithm are used to select the anchor frame to improve the quality of the initial anchor frame and the convergence speed of the model. The results show that the detection speed and accuracy of the proposed improved algorithm are superior to the existing methods,

reaching values of 83.9% and 98.9% respectively [9]. Huo has developed a real-time visual inspection system for misalignment detection of electronic components. In the system setup, the hardware part involves equipment setup, and the software part includes pre-processing and post-processing. In the pre-processing, image enhancement is performed to remove noise, and an improved YOLO model is used to detect defective elements. Experimental results show that the system can effectively detect missing components on the PCB board [10].

In summary, while existing PCB defect detection technologies such as traditional visual inspection, machine learning algorithms, and early deep learning models have made advances in automation and accuracy, they still face challenges such as speed and accuracy trade-offs, deployment challenges due to high model complexity, and lack of adaptability and robustness in complex environments. Especially for the high-precision detection of small defects, the existing technology still has room for improvement. To address these limitations, an innovative and improved YOLOv5s model is proposed, which integrates coordinate attention (CA), convolutional block attention mechanism (CBAM) and internal volume operator (IO), aiming to improve the accuracy and speed of detection, while reducing the computational burden of the model, making it more suitable for resource-constrained environments. This comprehensive technical approach demonstrates superior performance in ablation testing, significantly improving inspection accuracy while maintaining low inspection time and resource consumption, providing the electronics manufacturing industry with an efficient, accurate and easy-to-deploy PCB defect detection solution.

3. Method

To improve the detection performance of small defect PCBs, this study first optimizes the YOLOv5s network structure by combining CA and CBAM. Secondly, IO is introduced to improve the efficiency of feature extraction in the model and reduce the computational burden. Finally, a new PCBDD model is designed by combining CA, CBAM, and IO.

3.1. Optimization Design of YOLOv5s Network Architecture Combining CA and CBAM

In PCB defect detection and fault location, YOLOv5s was used as the backbone network to build the detection model. YOLOv5s combines high efficiency and high accuracy with excellent real-time detection capabilities, and its miniaturized design is suitable for resource-constrained environments while maintaining the optimized network structure and advanced performance of the YOLO series. In addition, YOLOv5s is highly flexible and scalable, enabling it to adapt to various customization improvements. YOLOv5s is the smallest model in the YOLOv5 model, which is mainly composed of Backbone, Neck and Head. The structure is shown in Figure 1 below [11].

In Figure 1, the Backbone in YOLOv5s includes four modules: Convolution Block (CBL), Focus, Cross Stage Partial (CSP), and Space Pyramid Pool (SPP). CBL is composed of Convolutional Layer (Conv), Batch Normalization (BN), and HardSwish. In addition, a Resunit residual module has been added to the CSP module. When using YOLOv5s to detect PCB defects, the sample is first input into the Focus module, which segments the data information into four parts and generates a dimension channel. Next, the partitioned information is input into CSP for processing and then input into the Path Aggregation Network (PanNet). This section includes several connecting layers, convolutional layers, and CSP layers. Finally, the detection results are output through the Head layer [12−13].

The study attempts to further achieve precise localization of small defects and fault targets in PCBs, while effectively aggregating deeper and broader contextual information to improve the feature extraction ability of the YOLOv5s. By utilizing two different attention mechanisms to optimize the YOLOv5s model, an improved YOLOv5s combining CA and CBAM, namely CA-CBAM-YOLOv5s, is proposed. Its structure is shown in Figure 2.

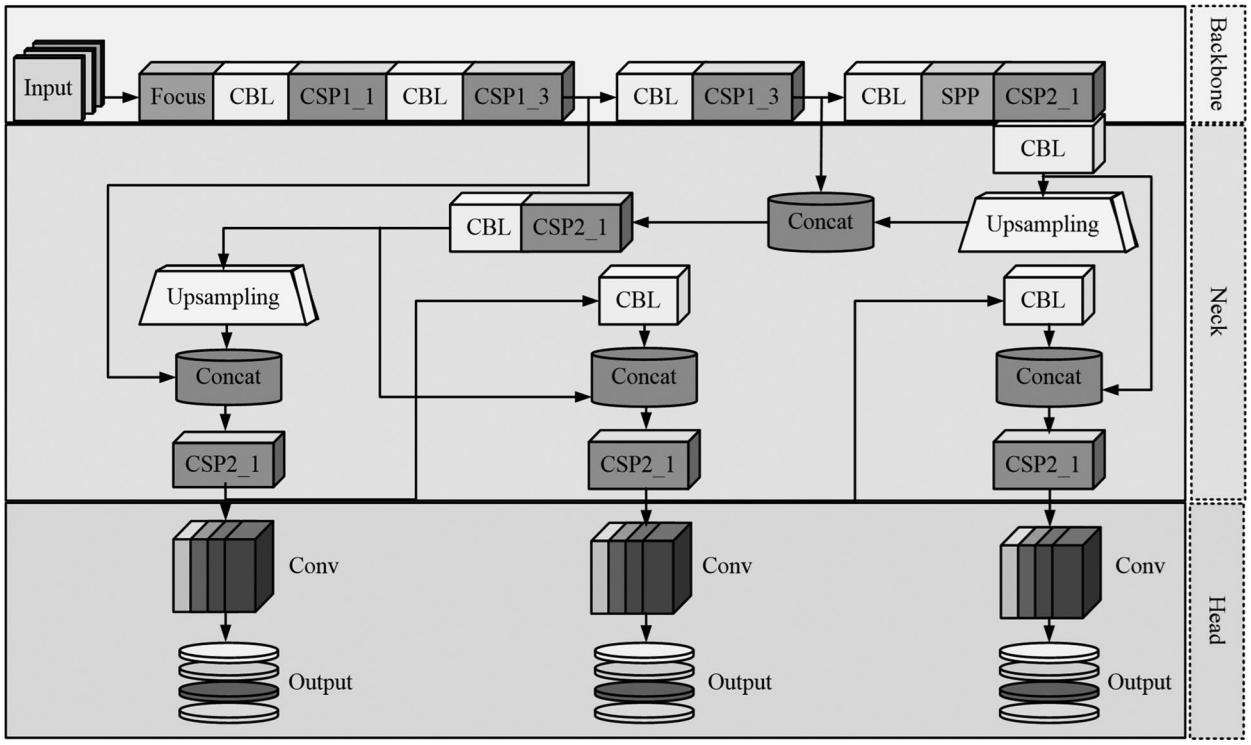

Figure 1. Structure of YOLOv5s.

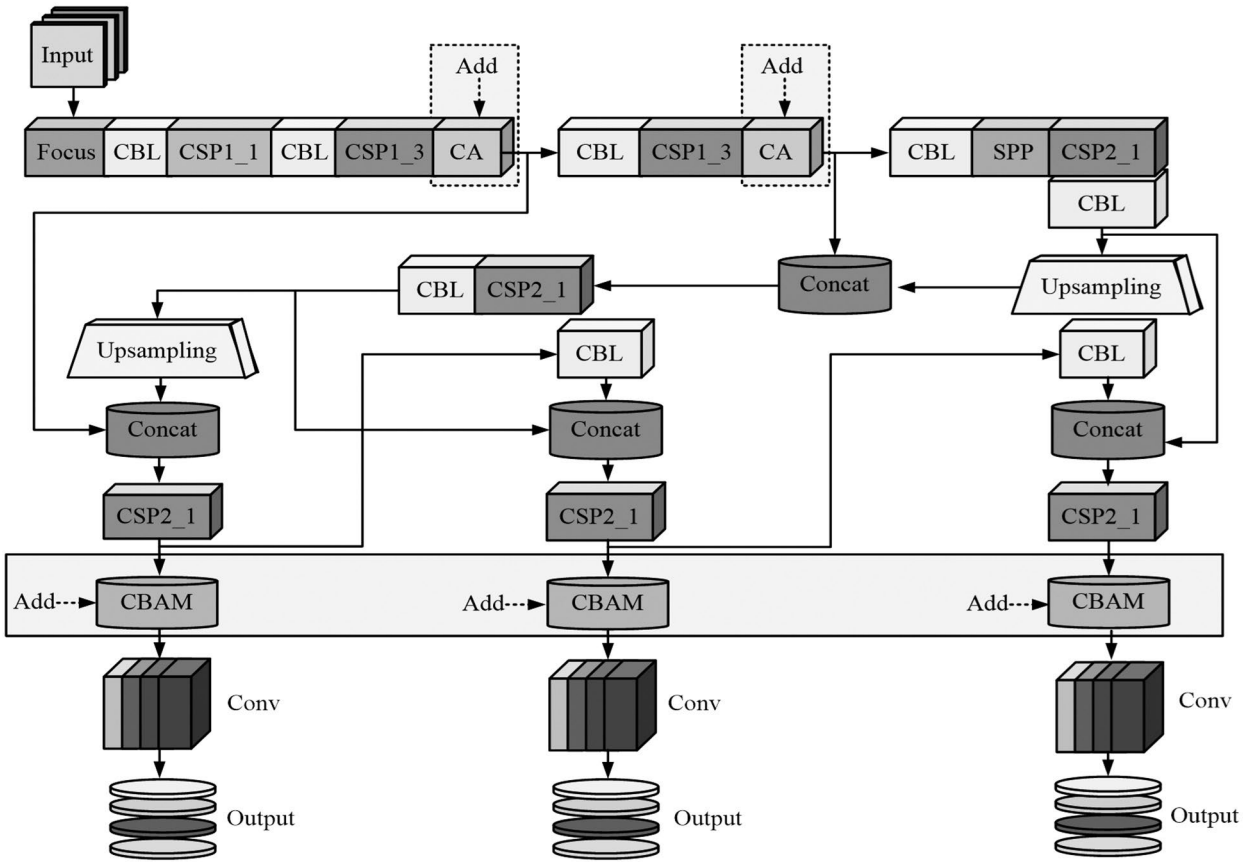

Figure 2. Structure of CA-CBAM-YOLOv7.

In Figure 2, this study first embeds two CA modules after CSP1-3 of Backbone to ensure that YOLOv5s preserves important defect location information during feature extraction. Meanwhile, three CBAM modules are embedded after the three CSP2-1 modules in the Neck section to improve the detection accuracy. Compared to other attention mechanisms, CA is relatively new. Its purpose is to capture the content of features in space in the spatial dimension, such as the spatial position and coordinates of features [14]. Figure 3 shows the CA structure.

In Figure 3, CA can be divided into two parts: embedding coordinate information and generating CA. The core of CA mechanism is to capture the spatial position information of features. It decomposes the global information into local features through pooling operations, thus preserving the spatial dimension information of features. CA consists of two main steps. The first step is to embed coordinate information and decompose input features into two directions by one-dimensional pooling operation. Secondly, coordinate attention is generated to enhance the expression ability of features through concatenation, convolution and nonlinear activation operations. In this way, CA can highlight important spatial location information and help the model locate defects more accurately. Assuming the dimension of input information is $C * H * W$, and each channel is denoted as x_c, the pooling decomposition formula is obtained as shown in equation (1) [15].

$$z_c = \frac{1}{H \times W} \sum_{a=1}^{H} \sum_{b=1}^{W} x_c(a,b) \tag{1}$$

In equation (1), H and W refer to the size of the pooling kernel. z_c represents global pooling. a and b are the input sizes of channel x_c in the spatial X and Y directions. After average pooling, $C * H * W$ can obtain the outputs of two new dimensions, $C * H * 1$ and $C * 1 * W$, while retaining a certain spatial positional relationship between these two outputs. The pooling information is concatenated using the formula shown in equation (2).

$$f = \delta(F_1[z^h, z^w]) \tag{2}$$

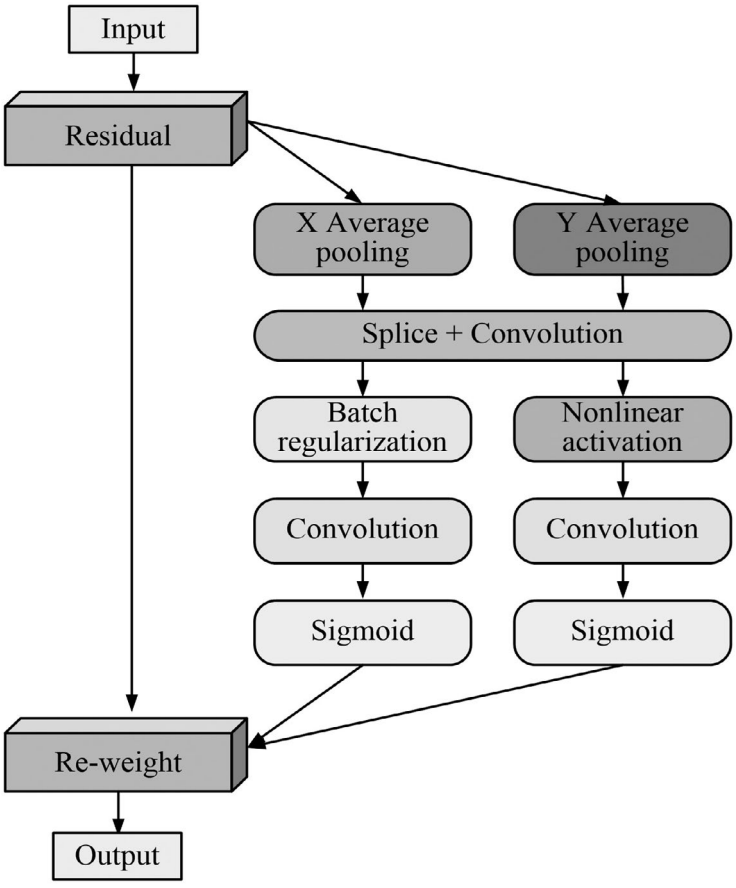

Figure 3. Structure of CA.

In equation (2), f means the spatial information of the input feature map after concatenation. $[z^h, z^w]$ is the pooling output of height h and width w in the spatial X and Y directions. F_1 is the convolutional transformation function. δ represents a nonlinear activation function. Decomposing f into f^h along the X direction to obtain the output weight of f^h is shown in equation (3).

$$g^h = \sigma(F_h(f^h)) \tag{3}$$

In equation (3), g^h is the attention weight acting in the X direction. F_h is the convolutional transformation function of f^h. σ is the sigmoid activation function. Similarly, f is decomposed into f^w along the Y direction, and the output weight of f^w is obtained as shown in equation (4).

$$g^w = \sigma(F_w(f^w)) \tag{4}$$

In equation (4), g^w is the attention weight acting in the Y direction. F_w is the convolutional transformation function of f^w. The output of CA can be obtained through equations (1) – (4) as shown in equation (5).

$$y_c(a, b) = x_c(a, b) \times g^h \times g^w \tag{5}$$

In equation (5), $y_c(a, b)$ is the output of the CA module. $x_c(a, b)$ is the input feature.

In order to improve the information extraction ability of the YOLOv5s model for small defect fault targets, this study added CBAM modules after three CSP2-1 modules. As a lightweight attention mechanism, CBAM not only has a smaller computational burden, but also has a larger kernel convolution to extract more features. This structure mainly consists of two parts: Channel Attention Mechanism (CAM) and Spatial Attention Mechanism (SAM), as shown in Figure 4 [16].

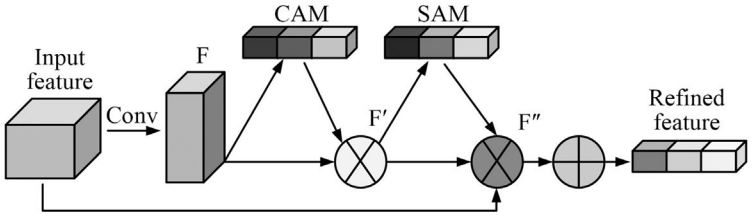

(a) CBAM structure diagram.

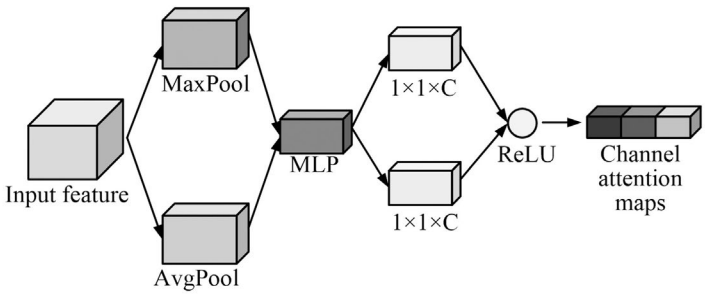

(b) Flowchart of feature processing in CAM.

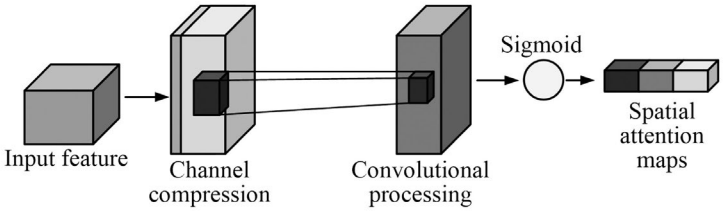

(c) Flowchart of feature processing in SAM.

Figure 4. Structure diagram of CBAM.

Figure 4 shows the structural diagrams of CBAM, CAM, and SAM. The purpose of CAM is to learn the features of different channels and weight them so that the model can focus on the channels with more information. SAM, on the other hand, focuses on identifying key regions in feature graphs, generating spatial attention graphs through convolution and activation functions. By combining these two kinds of attention, CBAM not only improves the representation ability of feature maps but also increases the sensitivity of the model to key features, thus improving the detection accuracy. In CBAM, its calculation formula is given in equation (6) [17].

$$F' = M_c(F) \otimes F \tag{6}$$

In equation (6), F is the feature map gained through the previous operation. $\otimes$ is the multiplication symbol between features. M_c is CAM. F' denotes the new feature map processed by CAM. The expression of the feature map processed by SAM is shown in equation (4).

$$F'' = M_s(F') \otimes F' \tag{7}$$

In equation (7), M_s represents SAM. F'' is the attention weight value obtained by processing F' through SAM. The final attention weight value is weighted and summed with the original feature map, and then output as a new feature map. In CAM, the formula for generating channel attention maps is given in (8).

$$MC(F) = \sigma\,(MLP(AvgPool(F)) + MLP(MaxPool(F))) \tag{8}$$

In equation (8), $MC(F)$ is the channel attention map. σ represents the ReLu activation function. MLP is a multi-layer perceptron. $AvgPool(F)$ and $MaxPool(F)$ are average and maximum pooling. In SAM, the formula for generating spatial attention maps is shown in equation (9).

$$MS(F) = \theta(f^{3*3}[AvgPool(F); MaxPool(F)]) \tag{9}$$

In equation (9), $MS(F)$ is the spatial-attention map. θ represents the activation function sigmoid. f^{3*3} is a convolution operation with a filter size of 3*3.

3.2. Construction of PCBDD Model Based on CA-CBAM-IO-YOLOv5s

After adding CA and CBAM modules, YOLOv5s can better extract small defects in PCBs, but it also increases the computational burden of the network. To reduce the parameter computation of CA-CBAM-YOLOv5s, this study introduces IO for optimization. IO is a new type of convolution operation aimed at improving the efficiency and flexibility of feature extraction. Traditional convolution operations achieve feature extraction by sliding a fixed convolution kernel over the input feature map. IO dynamically generates convolutional kernels to adapt to the features of each input position, making it more flexible and efficient [18–19]. Figure 5 shows the structure of IO.

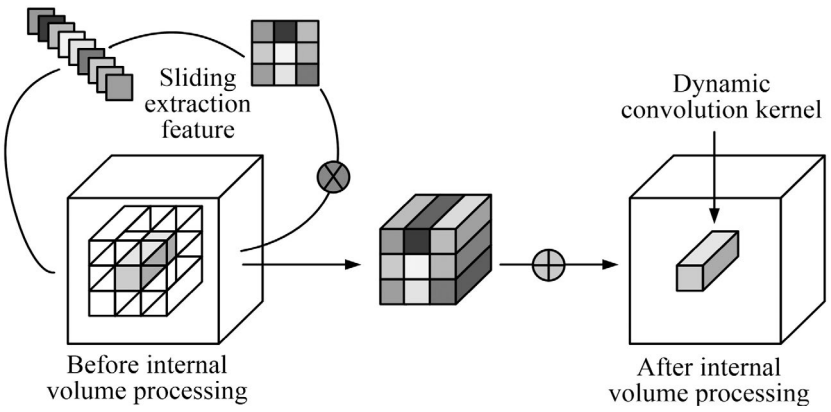

Figure 5. IO structure.

Figure 5 shows the inner convolution process of IO. Compared to traditional convolution operations, IO has the following four advantages. Firstly, IO dynamically generates convolution kernels based on the content of input features, which enables it to better capture local changes in input features and enhance feature expression capabilities. Secondly, compared to traditional convolution operations, the number of IO parameters is greatly reduced. This is because the convolution kernels generated by IO are specific to each position, rather than globally fixed, thereby reducing the quantity of parameters that need to be trained [20]. Thirdly, the computational complexity of IO is relatively low, which can reduce the computational burden of the model. Fourthly, IO performs well in processing input data with high heterogeneity, better adapting to different feature patterns, and improving robustness and generalization ability. In IO operations, ϕ represents the inner core, and the size of ϕ is denoted as $H \times W \times K \times K \times G$. ϕ refers to the execution of a convolutional kernel generation function on the input features to form a dynamic inner convolution core and ensure that the size of the core and the size of the input features are always aligned in the spatial dimension. The generating function of ϕ is shown in equation (10).

$$\phi\left(X_{i,j}\right) = \omega_1 \sigma(\omega_0 X_{i,j}) \tag{10}$$

In equation (10), $X_{i,j}$ represents the feature information input from position (i, j) to ϕ. ω_1 and ω_0 are two different feature mapping matrices,

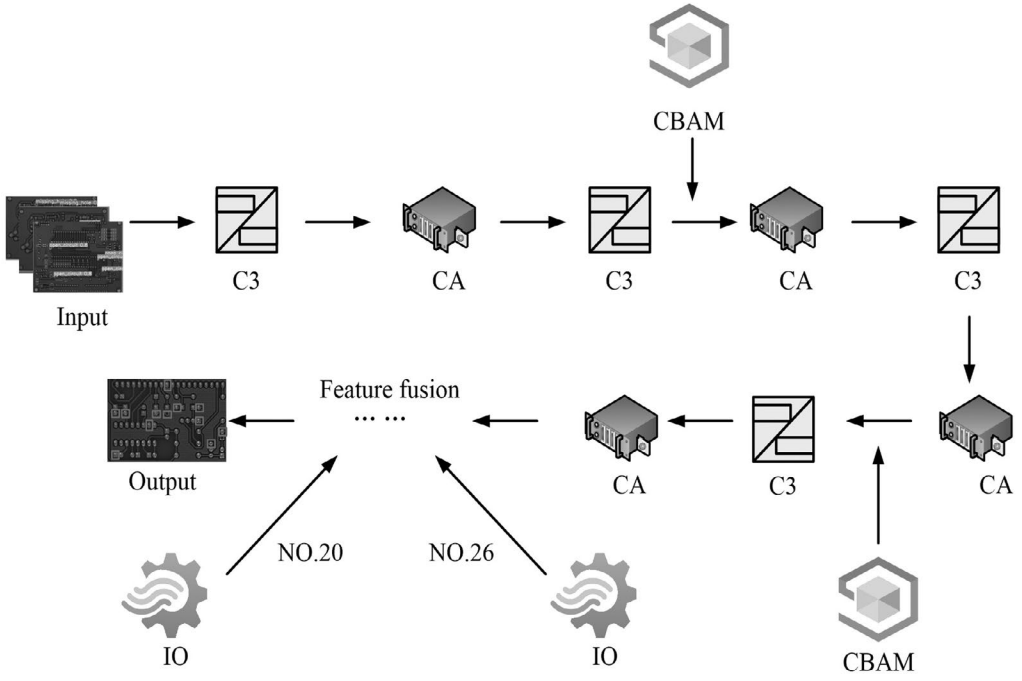

(a) Structure diagram of CA-CBAM-IO-YOLOv5s.

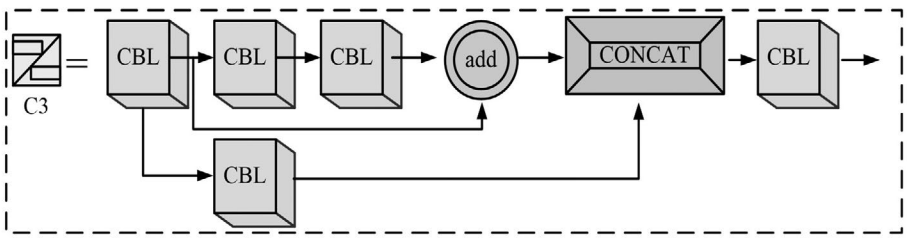

(b) Structure diagram of C3.

Figure 6. PCBDD frame structure.

and their specific expressions are shown in equation (11).

$$\begin{cases} \omega_0 \in R^{\frac{C}{r}\times C} \\ \omega_1 \in R^{\frac{C}{r}\times(K\times K\times G)} \end{cases} \tag{11}$$

In equation (11), r is the ratio seen by the channel. R represents a set of real numbers. G is the number of inner convolutional kernels shared by the channel. K is the size of the inner core. C is the number of unshared inner convolution kernels in the channel. The formula for inner convolution operation is given in equation (12).

$$y_{i,j} = \sum_{m=0}^{K-1}\sum_{n=0}^{K-1}\phi_{i,j}\left(X_{i+m,j+n}\right)\cdot X_{i+m,j+n} \tag{12}$$

In equation (12), $y_{i,j}$ is the output inner convolution operation value at position (i,j). $\phi_{i,j}(X_{i+m,j+n})$ is the generation function of the inner kernel at position (i, j). $X_{i+m, j+n}$ is the value of the input feature map at position $(i+m, j+n)$. m and n are the changes in coordinate positions in different directions. Figure 6 shows the framework for PCBDD using CA-CBAM-IO-YOLOv5s.

In Figure 6, YOLOv5s serves as the backbone network and adds a CA module after each C3 module. Four CA modules have been added in total. Due to the introduction of the CBAM module increasing computational complexity, the detection speed slows down. Therefore, to ensure real-time performance as much as possible, the network only retains two CBAMs to reduce the computational load of the model. Finally, IO is embedded in the 20th and 26th layers of the network, respectively, and an improved model, CA-CBAM-IO-YOLOv5s, is ultimately formed. When using the CA-CBAM-IO-YOLOv5s model for PCBDD, the PCB image is first input into the model, and after processing by the backbone network, the CA mechanism embedded after each C3 module enhances the feature expression ability. Subsequently, the model further optimizes feature extraction and improved detection accuracy by inserting two CBAM modules in the neck region. The IO embedded in the 20th and 26th layers will improve computational efficiency and reduce parameters by dynamically generating convolutional kernels. Finally, the model outputs detection results containing defect types and positions, achieving efficient and accurate detection of PCB surface and internal defects [21].

Based on the above content, IO has been innovatively integrated into YOLOv5s model to improve the efficiency and flexibility of feature extraction by significantly reducing the number of parameters and computational complexity compared with traditional convolution through its dynamic convolution kernel generation capability. In the YOLOv5s architecture, IO is embedded at layers 20 and 26 of the network, an integrated strategy that not only optimizes feature representation, but also maintains the real-time performance of the model. Through this integration, IO helps .the model to better adapt to local changes in input characteristics, while maintaining a balance of detection accuracy and speed, making the improved CA-CBAM-IO-YOLOv5s model perform well in PCB defect detection tasks.

4. Results and Discussion

To demonstrate the good performance of the CA-CBAM-IO-YOLOv5s model, this study first used ablation experiments to test the benchmark performance among various combinations of the model. Secondly, Single Shot Multi-Box Detector (SSD), YOLOv5s, and Mask Region-Based CNN (Mask-RCNN) were selected as comparison algorithms to test their detection performance. Finally, four detection models were constructed using different algorithms to verify the CA-CBAM-IO-YOLOv5s in practical defect PCB detection applications.

4.1. Performance Testing of CA-CBAM-IO-YOLOv5s Algorithm

The PCB dataset selected for the study was sourced from Peking University and contained 693 high-resolution images covering six common defect types: leaky hole, rat bite, open circuit, short circuit, stray and stray copper. The number of defects in the image is balanced, the average area ratio is small, and the aspect ratio is close to 1, which is suitable for small target detection. The dataset was labeled in YOLO format and expanded by Music online enhancement strategy to enhance model

generalization. In the experiment, the initial learning rate was set to 0.001, the batch size was set to 16, and the training period was initially set to 50 epochs. The size of the anchor box obtained using clustering is assumed to be (12, 16), (24, 32), (32, 24). The voidage of the voidage convolution starts from 1. The selected optimizer was Adam, whose β1 and β2 are set to 0.9 and 0.999 respectively. SSD, YOLOv5s and Mask-RCNN are selected as comparison algorithms in the experiment, because they are representative advanced algorithms in the field of object detection, which can provide performance benchmarks and comprehensively evaluate the effectiveness of new algorithms. Each of these algorithms has its own characteristics, covering single-stage to multi-stage detection methods, and helps to comprehensively measure the performance of the newly proposed CA-CBAM-IO-YOLOv5s model in terms of accuracy, speed, and application potential. By comparing with these well-known algorithms, the innovation and practical application value of the new model can be demonstrated more intuitively.

Considering that the CA-CBAM-IO-YOLOv5s model is composed of multiple different modules, different combination methods are chosen to test the ablation performance of the model. The detection accuracy (precision), recall rate and F1 value are selected as the detection indexes of ablation experiment. Among them, precision ensured the accuracy of the model in predicting the positive class and avoided misjudging the flawless PCB. The recall rate ensures that the model can detect as many actual defects as possible, reducing missed tests; The F1 value balances precision and recall to provide a comprehensive performance indicator. The results of ablation experiments are shown in Table 1.

Table 1 lists a total of five different network combinations, denoted as M1, M2, M3, M4, and M5. Among them, M5 is the final CA-CBAM-IO-YOLOv5s detection model built. Among the five different combinations, M3 has the worst benchmark performance test results, with precision, recall, and F1 values of 0.864, 0.858, and 0.861, respectively. The benchmark performance of M5 combination is the best, with three values of 0.978, 0.986, and 0.983, respectively. Ablation results showed that all components in the CA-CBAM-IO-Yolov5S model could promote the detection performance. Specifically, the single attention mechanism CA or CBAM could already improve the model performance, but the effect was better when combined. Although the internal volume operator IO has limited performance improvement when used alone, it can significantly reduce the computational burden and increase the processing power when combined with the attention mechanism. The final model CA-CBAM-IO-YOLOv5s shows excellent performance in precision, recall rate and F1 value, which proves that the model combining these technologies can effectively deal with the defect image with large amount of data while maintaining high detection accuracy. After completing the ablation test, this study compares the loss curve changes of SSD, YOLOv5s, Mask-RCNN, and CA-CBAM-IO-YOLOv5s in the training and testing sets, as exhibited in Figure 7.

Table 1. Ablation test results of CA-CBAM-IO-YOLOv5s model.

Network structure	Precision	Recall	F1
CA+YOLOv5s (M1)	0.862	0.885	0.876
CBAM+YOLOv5s (M2)	0.889	0.893	0.890
IO+YOLOv5s (M3)	0.864	0.858	0.861
CA+CBAM+YOLOv5s (M4)	0.942	0.957	0.955
CA+CBAM+IO+YOLOv5s (M5)	0.978	0.986	0.983

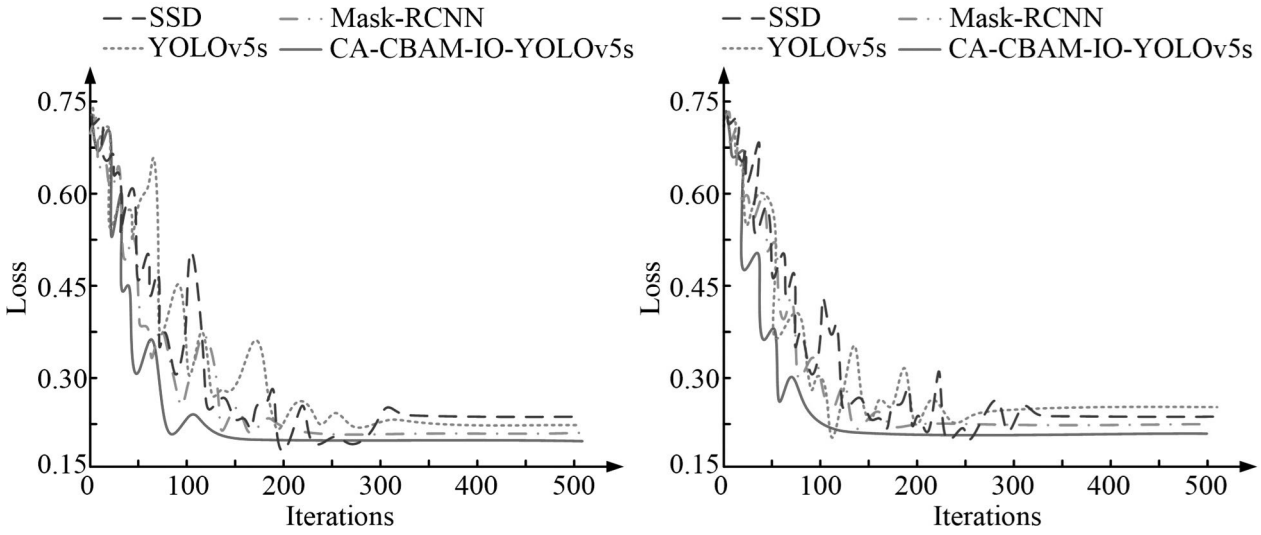

(a) Loss curve in training set. *(b)* Loss curve in the test set.

Figure 7. The loss curves of the four algorithms under two data sets.

In Figure 7 (a), all four algorithms exhibit varying degrees of iterative fluctuations during the algorithm process. Compared to SSD, YOLOv5s, and Mask-RCNN, CA-CBAM-IO-YOLOv5s has a smaller fluctuation amplitude and can reach a stable state in the training set with only 136 iterations, while the other three models require 328, 336, and 225 iterations. Similarly, in Figure 7 (b), the four algorithms can be iterated 331 times, 273 times, 186 times, and 112 times, respectively, to complete the iteration and maintain a stable loss value. By comparing the error performance of four algorithms during the training process, the Mean Squared Error (MSE) and Mean Absolute Error (MAE) curves shown in Figure 8 are obtained.

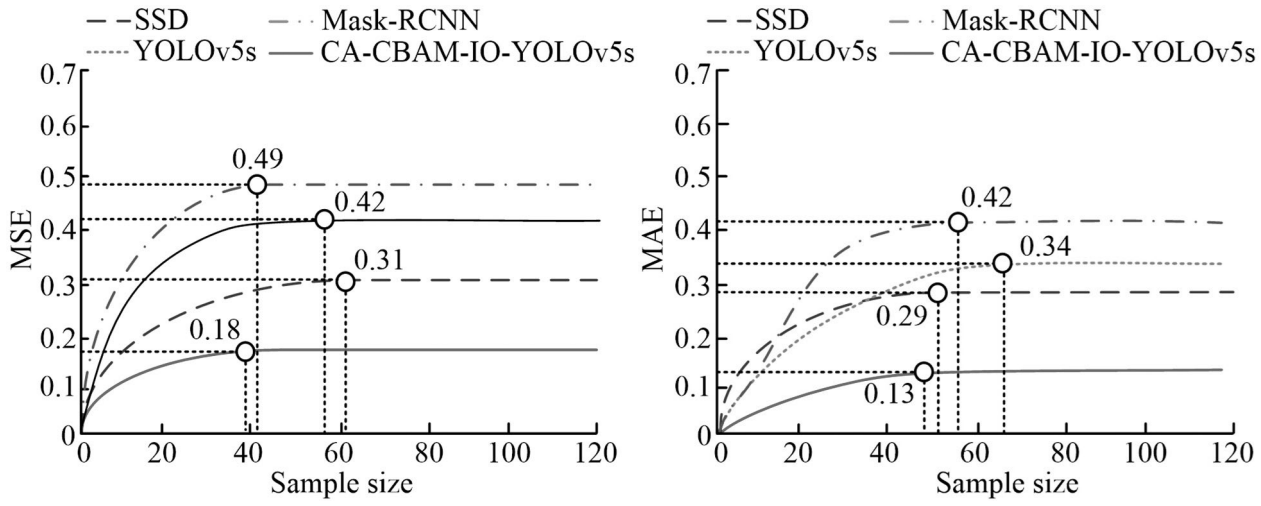

(a) The results of MSE. *(b)* The results of MAE.

Figure 8. The MSE and MAE values of the four algorithms.

In Figure 8 (a), when SSD, YOLOv5s, Mask-RCNN, and CA-CBAM-IO-YOLOv5s reach a stable state, the MSE values of the four algorithms are 0.49, 0.42, 0.31, 0.18, and the MAE values are 0.42, 0.34, 0.29, and 0.13. The research algorithm can obtain stable MSE values at a faster speed and has better error performance. This is because the CA and CBAM structures in the model can enhance the main network model YOLOv5s's ability to extract detailed features, thereby better avoiding missed and false detections. Image Ambiguity (IA) and Structural Similarity Loss (SSL) are used as detection metrics. The lower the IA value, the lower the ambiguity of the algorithm in the detection process [22]. The smaller the SSL value, the more complete the image features are preserved during the detection process, and the lower the damage to the overall image structure. Figure 9 shows the IA and SSL values of four algorithms during testing.

In the IA values shown in Figure 9 (a), when the sample size increased from 0 to 400, the IA values of the three comparison algorithms fluctuate significantly, but the IA values of the study algorithms remain below 0.2. Throughout the training process, the maximum IA values of SSD, YOLOv5s, Mask-RCNN, and CA-CBAM-IO-YOLOv5s are 0.65, 0.59, 0.32, and 0.18. In Figure 9 (b), the maximum SSL values of the four algorithms during training are 0.67, 0.61, 0.28, and 0.20, respectively.

4.2. Analysis of the Practical Application Effect of the CA-CBAM-IO-YOLOv5s Model

In addition to testing the performance of four comparative models, SSD, YOLOv5s, Mask-RCNN, and CA-CBAM-IO-YOLOv5s, this study also selects five types of PCBs with different defect appearances, including leakage defects, open circuit defects, short circuit defects, burr defects, and bite defects, as the detection objects. Table 2 further tests the performance of the four models in actual detection tasks.

Table 2 shows the accuracy and time for detecting five types of defective PCBs, with the research model's being the highest among them. When detecting open circuit defects in PCBs, the mean detection accuracy of the CA-CBAM-IO-YOLOv5s can reach 99.02%. In addition, the average detection time of this model is also lower than the other three, with a minimum of 0.08 seconds to complete the detection task.

Figures 10 (a) to (d) show the actual performance of four models in detecting a defective PCB. Based on Figure 10, SSD, YOLOv5s, Mask-RCNN, and CA-CBAM-IO-YOLOv5s can detect 6, 7, 8, and 12 defective components, respectively. In summary, the research model has a wider detection range for defective PCBs and can accurately detect more defective electronic components.

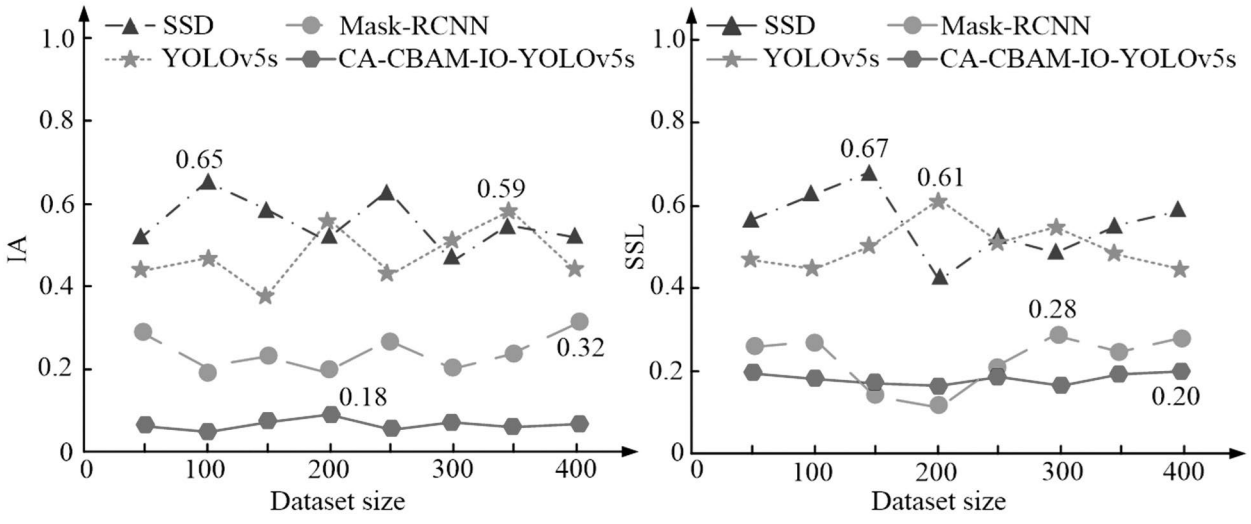

(a) IA test result. *(b)* SSL test results.

Figure 9. Four algorithms for detecting IA and SSL values of different numbers of samples.

Table 2. The detection effect of various models for different defective PCB.

PCB type	Network structure	Average detection accuracy/%	Average detection time/s
Leaky defect	SSD	86.38%	0.56
	YOLOv5s	89.43%	0.34
	Mask-RCNN	92.91%	0.25
	CA-CBAM-IO-YOLOv5s	98.25%	0.13s
Open circuit defect	SSD	87.08%	0.68
	YOLOv5s	88.79%	0.45
	Mask-RCNN	93.89%	0.22
	CA-CBAM-IO-YOLOv5s	99.02%	0.11s
Short-circuit defect	SSD	87.89%	0.48
	YOLOv5s	91.01%	0.35
	Mask-RCNN	94.26%	0.21
	CA-CBAM-IO-YOLOv5s	98.94%	0.09s
Burr defect	SSD	87.12%	0.50
	YOLOv5s	89.56%	0.44
	Mask-RCNN	93.28%	0.23
	CA-CBAM-IO-YOLOv5s	98.16%	0.08s
Occlusal defect	SSD	85.04%	0.61
	YOLOv5s	89.71%	0.49
	Mask-RCNN	92.36%	0.27
	CA-CBAM-IO-YOLOv5s	97.89%	0.16s

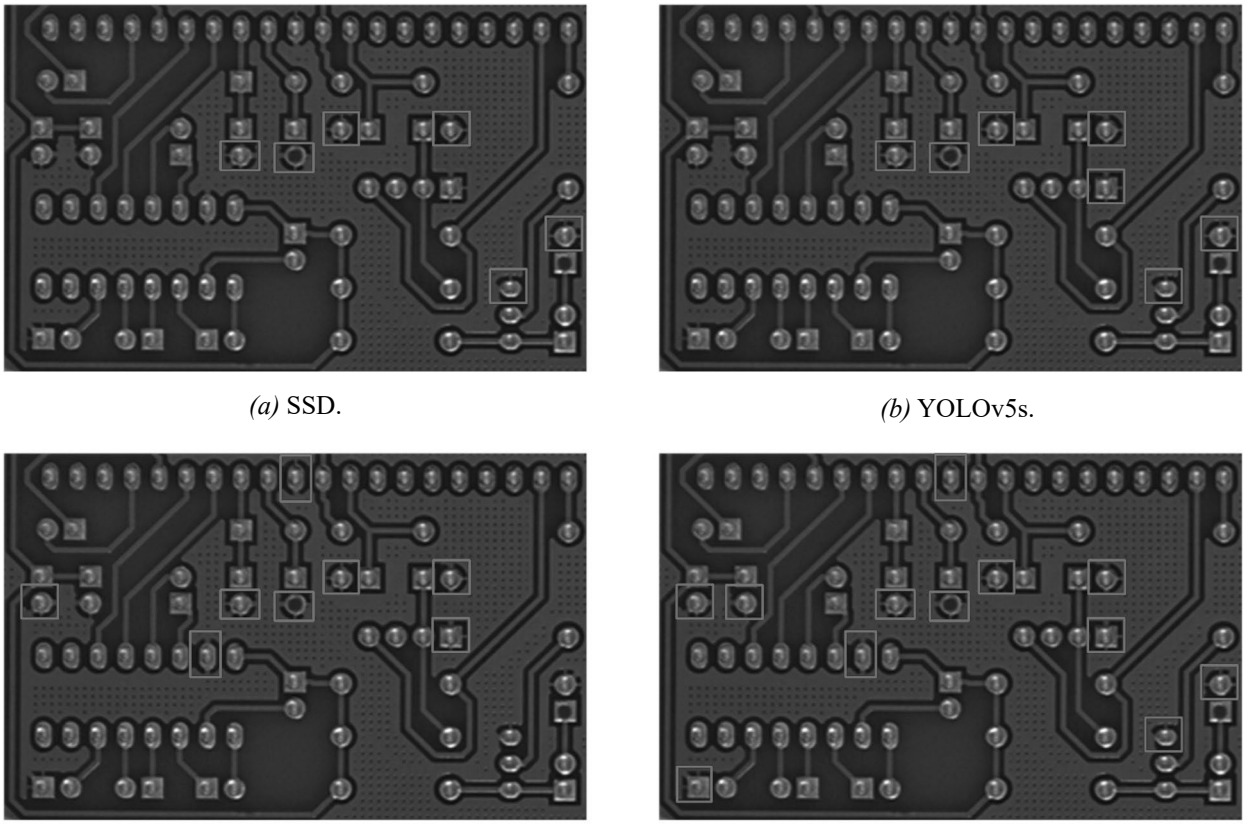

(a) SSD. *(b)* YOLOv5s. *(c)* Mask-RCNN. *(d)* CA-CB AM-IO-YOLOv5s.

Figure 10. Recognition effects of different models.

5. Discussion

The proposed CA-CBAM-IO-YOLOv5s model performs well in PCB defect detection tasks, and its advantages can be attributed to several key innovations. First of all, the introduction of coordinate attention mechanism (CA) and convolutional attention mechanism (CBAM) significantly improved the ability of the model to capture small flaw features. CA enhanced the sensitivity of the model to the location of defects by embedding spatial position information. CBAM, on the other hand, enhances the representation power of feature maps through fine channel and spatial attention mechanism. Moreover, the addition of the IO operator further optimizes the computational efficiency of the model, reduces the number of parameters, and enables the model to maintain high accuracy while having faster detection speed.

However, despite the remarkable results achieved in the experiment, the model still has some limitations, such as the imbalanced sensitivity to specific defect types and the ability to generalize under complex environmental conditions. Future work needs to further fine-tune the model to achieve wider applicability and greater robustness. In addition, the model has a broad application prospect in the field of PCB manufacturing and quality control, which can not only improve the efficiency and accuracy of automated inspection, but also has the potential to promote the innovation and development of quality control in the entire electronics manufacturing industry. With the continuous progress of technology and the optimization of models, its role in actual production will become more and more important, providing a stronger guarantee for the quality and reliability of electronic products.

6. Conclusion

In this study, an enhanced YOLOv5s model is proposed, which combines CA, CBAM and IO mechanisms to achieve efficient and accurate PCB defect detection. The proposed CA-CBAM-IO-YOLOv5s model performs well in detecting various PCB defects, achieving high accuracy (precision, 97.8%), recall rate (98.6%) and F1 score (98.3%). The model is capable of detecting small defects with high accuracy while maintaining low computational complexity, making it a promising solution for industrial PCB inspection processes. The integration of CA and CBAM mechanisms significantly improves the feature extraction capability of the model, especially for small defects, while the IO mechanism effectively reduces the computational burden. These enhancements allow the model to outperform existing state-of-the-art methods in both accuracy and efficiency. While the current study focused on five common PCB defect types, future research should explore the model's performance across a wider range of defects and PCB designs. In addition, the robustness of the study model under different imaging conditions and its potential in real-time detection systems can further enhance its practical applicability. In summary, the CA-CBAM-IO-YOLOv5s model represents a significant advance in automated PCB defect detection, providing a powerful tool for improving quality control in the electronics manufacturing process.

References

[1] S. A. Singh and K. A. Desai, "Automated Surface Defect Detection Framework using Machine Vision and Convolutional Neural Networks", *Journal of Intelligent Manufacturing*, vol. 34, no. 4, pp. 1995–2011, 2023. https://doi.org/10.1007/s10845-021-01878-w

[2] Z. Ren *et al.*, "State of the Art in Defect Detection Based on Machine Vision", *International Journal of Precision Engineering and Manufacturing-Green Technology*, vol. 9, no. 2, pp. 661–691, 2022. https://doi.org/10.1007/s40684-021-00343-6

[3] S. Liu *et al.*, "Circuit Welding Defect Detection Method Based on Metric Learning", *Transactions of Beijing institute of Technology*, vol. 44, no. 6, pp. 625–634, 2024. https://doi.org/10.15918/j.tbit1001-0645.2023.181

[4] Z. Yu *et al.*, "A Lightweight and Efficient Model for Surface Tiny Defect Detection", *Applied Intelligence*, vol. 53, no. 6, pp. 6344–6353, 2023. https://doi.org/10.1007/s10489-022-03633-x

[5] Y. Li *et al.*, "Attention-guided Multiscale Neural Network for Defect Detection in Sewer Pipelines", *Computer-Aided Civil and Infrastructure Engineering*, vol. 38, no. 15, pp. 2163–2179, 2023. https://doi.org/10.1111/mice.12991

[6] G. Zhou *et al.*, "Lightweight PCB Defect Detection Algorithm Based on MSD-YOLO", *Cluster Computing*, vol. 27, no. 3, pp. 3559–3573 , 2024. https://doi.org/10.1007/s10586-023-04156-x

[7] A. Sezer and A. Altan, "Detection of Solder Paste Defects with an Optimization-based Deep Learning Model using Image Processing Techniques", *Soldering & Surface Mount Technology*, vol. 33, no. 5, 291–298, 2021. https://doi.org/10.1108/ssmt-04-2021-0013

[8] Y. Long *et al.*, "PCB Defect Detection Algorithm Based on Improved YOLOv8", *Academic Journal of Science and Technology*, vol. 7, no. 3, pp. 297–304, 2023. https://doi.org/10.54097/ajst.v7i3.13420

[9] Y. Xie *et al.*, "Surface Defect Detection Algorithm Based on Feature-enhanced YOLO", *Cognitive Computation*, vol. 15, no. 2, pp. 565–579, 2023. https://doi.org/10.1007/s12559-022-10061-z

[10] X. Huo, "Development of a Real-time Printed Circuit Board (PCB) Visual Inspection System Using You Only Look Once (YOLO) and Fuzzy Logic Algorithms", *Journal of Intelligent & Fuzzy Systems*, vol. 45, no. 3, pp. 4139–4145, 2023. https://doi.org/10.3233/JIFS-223773

[11] L. Ang *et al.*, "CSSD-YOLO: A Modified YOLOv5 Method for Solder Joint Defect Detection", *Journal of Advanced Research in Applied Sciences and Engineering Technology*, vol. 31, no. 3, pp. 249–264, 2023. https://doi.org/10.37934/araset.31.3.249264

[12] M. Chakraborty *et al.*, "Electronic Waste Reduction Through Devices and Printed Circuit Boards Designed for Circularity", *IEEE Journal on Flexible Electronics*, vol. 1, no. 1, pp. 4–23, 2022. https://doi.org/10.1109/JFLEX.2022.3159258

[13] G. Lakshmi *et al.*, "A Survey of PCB Defect Detection Algorithms", *Journal of Electronic Testing*, vol. 39, no. 5, pp. 541–554, 2023. https://doi.org/10.1007/s10836-023-06091-6

[14] X. Wu *et al.*, "Multiple Detection Model Fusion Framework for Printed Circuit Board Defect Detection", *Journal of Shanghai Jiaotong University (Science)*, vol. 28, no. 6, pp. 717–727, 2023. https://doi.org/10.1007/s12204-022-2471-0

[15] Y. Chang *et al.*, "PCB Defect Detection Based on PSO-optimized Threshold Segmentation and SURF Features", *Signal, Image and Video Processing*, vol. 18, no. 5, pp. 4327–4336, 2024. https://doi.org/10.1007/s11760-024-03075-7

[16] Q. Zhao *et al.*, "PCB Surface Defect Fast Detection Method Based on Attention and Multi-source Fusion", *Multimedia Tools and Applications*, vol. 83, no. 2, pp. 5451–5472, 2024. https://doi.org/10.1007/s11042-023-15495-7

[17] K. Zhang, "Using Deep Learning to Automatic Inspection System of Printed Circuit Board in Manufacturing Industry Under the Internet of Things", *Computer Science and Information Systems*, vol. 20, no. 2, pp. 723–741, 2023. https://doi.org/10.2298/CSIS220718020Z

[18] F. Chen *et al.*, "NHD-YOLO: Improved YOLOv8 Using Optimized Neck and Head for Product Surface Defect Detection with Data Augmentation", *IET Image Processing*, vol. 18, no. 7, pp. 1915–1926, 2024. https://doi.org/10.1049/ipr2.13073

[19] Y. Wan and J. Li, "LGP-YOLO: An Efficient Convolutional Neural Network for Surface Defect Detection of Light Guide Plate", *Complex & Intelligent Systems*, vol. 10, no. 2, pp. 2083–2105, 2024. https://doi.org/10.1007/s40747-023-01256-4

[20] S. N. I. Zulkeefli and N. Hashim, "Comparison of CNN-based Algorithms for Halal Logo Recognition", *Journal of System and Management Sciences*, vol. 12, no. 5, pp. 155–168, 2022. https://doi.org/10.33168/JSMS.2022.0510

[21] I. H. Jung *et al.*, "Advanced Smart Parking Management System Development Using AI", *Journal of System and Management Sciences*, vol. 12, no. 1, pp. 3–62, 2022. https://doi.org/10.33168/JSMS.2022.0105

[22] H. M. Khan *et al.*, "A Review on Quality of Service Monitoring, Violation and Remediation for the Cloud", *Journal of System and Management Sciences*, vol. 13, no. 5, pp. 107–126, 2023. https://doi.org/10.33168/JSMS.2023.0507

Received: July 2024
Revised: August 2024
Accepted: September 2024

Contact address:
Zhijun Xiao
School of Electrical and Electronic Information Engineering
Hubei Polytechnic University
Huangshi
Hubei
China
e-mail: xzj202212@163.com

Zhijun Xiao holds a Master's degree, which he obtained in June 2012 from Hubei Polytechnic University. Currently, he serves as a Lecturer in the field of Electronic Engineering, leveraging his academic expertise and practical knowledge to contribute to the field.